J. Dairy Sci. 105
https://doi.org/10.3168/jds.2022-22008
© 2022, The Authors. Published by Elsevier Inc. and Fass Inc. on behalf of the American Dairy Science Association®.
This is an open access article under the CC BY license (http://creativecommons.org/licenses/by/4.0/).

Lactobacillus reuteri-fortified camel milk infant formula: Effects of encapsulation, in vitro digestion, and storage conditions on probiotic cell viability and physicochemical characteristics of infant formula

Mariam Algaithi,[1]* Priti Mudgil,[1]* Marwa Hamdi,[1] Ali Ali Redha,[2,3] Tholkappiyan Ramachandran,[4] Fathala Hamed,[4] and Sajid Maqsood[1,5]†
[1]Department of Food Science, College of Agriculture and Veterinary Medicine, United Arab Emirates University, Al Ain 15551, United Arab Emirates
[2]Department of Public Health and Sport Sciences, College of Life and Environmental Sciences, University of Exeter, Exeter EX1 2LU, United Kingdom
[3]Centre for Nutrition and Food Sciences, Queensland Alliance for Agriculture and Food Innovation, University of Queensland, Brisbane QLD 4072, Queensland, Australia
[4]Department of Physics, College of Science, United Arab Emirates University, Al Ain 15551, United Arab Emirates
[5]Zayed Centre of Health Science, United Arab Emirates University, Al Ain 15551, United Arab Emirates

ABSTRACT

Lactobacillus reuteri fortified camel milk infant formula (CMIF) was produced. The effect of encapsulation in different matrices (sodium alginate and galacto-oligosaccharides) via spray drying, simulated infant gastrointestinal digestion (SIGID), and storage conditions (temperature and humidity) on the viability of *L. reuteri* in CMIF and the physicochemical properties of CMIF were evaluated. Compared with free cells, probiotic cell viability was significantly enhanced against SIGID conditions upon encapsulation. However, *L. reuteri* viability in CMIF decreased after 60 d of storage, predominantly at higher storage humidity and temperature levels. At the end of the storage period, significant changes in the color values were observed in all CMIF, with a reduction in their greenness, an increase in yellowness, and a wide variation in their whiteness. Moreover, pH values and caking behavior of all CMIF stored at higher temperature (40°C) and humidity [water activity (a_w) = 0.52] levels were found to be significantly higher than the samples stored under other conditions. Over 30 d of storage at lower humidity conditions (a_w = 0.11 and 0.33) and room temperature (25°C), no significant increase in CMIF lipid oxidation rates was noted. Fourier-transform infrared spectroscopy analysis showed that, compared with the other storage conditions, CMIF experienced fewer changes in functional groups when stored at a_w = 0.11. Microscopic images showed typical morphological characteristics of milk powder, with round to spherical-shaped particles. Overall, camel milk fortified with encapsulated *L. reuteri* can be suggested as a promising alternative in infant formula industries, potentially able to maintain its physicochemical characteristics as well as viability of probiotic cells when stored at low humidity levels (a_w = 0.11) and temperature (25°C), over 60 d of storage.
Key words: camel milk infant formula, encapsulation, probiotic viability, physicochemical characteristics

INTRODUCTION

Human milk is considered infants' main source of nutrients, providing them with well-balanced nutrition and protection against illnesses (Martin et al., 2016; Savarino et al., 2021). When mother's milk is unavailable, infant milk formula (**IMF**) products are used as a substitute for human milk. Formulas can provide the required nutritional needs until infants become used to complementary foods (Byrne et al., 2021; Mudgil et al., 2022).

Infant milk formulas are commonly made from bovine milk; however, bovine milk contains β-LG, which is the main allergenic protein of bovine milk for infants. Advantageously, camel milk is β-LG-free, which could make it a good substitute for bovine milk to avoid infant allergies, and thereby a suitable source for IMF production (Momen et al., 2019). In fact, the immunoglobulins present in camel milk are similar to those in human breast milk, thus reducing children's allergic reactions and strengthening their immune system (Zibaee et al., 2015; Muthukumaran et al., 2022). Upon digestion, camel milk proteins could be hydrolyzed with the digestive enzymes into bioactive hydrolysates with a wide range of nutraceutical and pharmacological activities (Ali Redha et al., 2022). Most commercially available IMF products are powders, and they should ideally

Received February 23, 2022.
Accepted June 24, 2022.
*These authors contributed equally to this work.
†Corresponding author: sajid.m@uaeu.ac.ae

maintain acceptable physical and compositional stability during transportation and storage. Lipid oxidation, Maillard reaction, lactose crystallization, and caking are all caused by instability of IMF powders. These defects are linked to the product's composition and storage conditions (i.e., temperature, relative humidity, and time). To extend the shelf life of IMF powders, a good understanding of the effects of storage conditions on their physicochemical properties, surface properties, and stability is required (Wazed and Farid, 2022).

Moreover, for improved infant health, probiotic fortification of infant formula has been reported to improve intestinal microbial balance, which will benefit infants' general health. Probiotics are considered live microorganisms that can provide health benefits to the host when they are consumed in sufficient amounts (Binda et al., 2020). A minimum of 10^8 colony-forming units (cfu) per milliliter or gram of probiotic food is recommended at the time of ingestion (Hill et al., 2014). Most frequent probiotics are bacteria from the genera *Lactobacillus* and *Bifidobacterium* (Kaźmierczak-Siedlecka et al., 2021). Different studies have indicated that infant formula supplemented with probiotic bacteria has shown no safety concerns or adverse effects on infant growth (Vandenplas et al., 2017). Maldonado et al. (2019) reported that the consumption of formula milk powder fortified with *Lactobacillus fermentum* CECT5716 or *Lactobacillus rhamnosus* GG by breastfed infants (0–6 mo) was well tolerated and did not show any adverse effects on infants' normal growth. More recently, Chi et al. (2020) suggested that infant formula containing *Bifidobacterium lactis* positively modulates the composition, stability, and function of the gut microbiota of low-weight newborns.

Different factors can affect the stability of probiotics in food products and formulation, such as food properties, processing parameters, and microbial parameters (Terpou et al., 2019). Three key challenges that probiotics face before reaching the gut mucosa are the acidity of the stomach, the presence of digestive enzymes, and bile salts in the upper intestine (Zhang et al., 2015; Markowiak and Slizewska, 2017). To overcome these issues of probiotic stability, microencapsulation is often presented as one of the most effective techniques for improving the stability of probiotics, not only during processing and storage but also to ensure their activity within the gut (Yao et al., 2020). Complex carbohydrates and alginate are the most used wall material reported for microencapsulation of probiotic bacteria (Motalebi Moghanjougi et al., 2021). Prebiotics in infant nutrition, such as human milk oligosaccharides, promote the growth of microorganisms already present in the large intestine. The most likely prebiotic in human milk that encourages the growth of bifidobacteria in the infant's intestine has been identified as complex neutral oligosaccharides (Walsh et al., 2020).

To the best of our knowledge, the formulation of infant formula from camel milk has only been recently studied (Mudgil et al., 2022; Zou et al., 2022). Moreover, there is no research or literature on the fortification of probiotic bacteria in camel milk-based infant formula, and even fewer studies exist on the survivability and stability of probiotic organisms during storage and simulated digestion. Therefore, this study focuses on the production of encapsulated and non-encapsulated *Lactobacillus reuteri*-fortified camel milk infant formula (**CMIF**), and the exploration of the effects of simulated infant gastrointestinal digestion (**SIGID**) and different storage conditions (relative humidity and temperature) on the viability of *L. reuteri* and the physicochemical characteristics of CMIF.

MATERIALS AND METHODS

No animals were used in this study, and ethical approval for the use of animals was thus deemed unnecessary.

Chemicals and Reagents

Camel milk (**CM**) powders with a composition of 26% fat, 41% carbohydrates, 26% protein, 926 mg of calcium, and 1% sodium, were obtained from Al Ain Dairy Farm (Camelait, Al Ain Farms, Al Ain, United Arab Emirates).

Lactose, de Man, Rogosa, and Sharpe (**MRS**) broth, bacteriological-grade agar powder, and bacteriological peptone were purchased from HiMedia Laboratories. Daily multivitamins and minerals (Now Foods), lithium chloride (Merck), magnesium chloride (VWR Chemicals BDH), magnesium nitrate (Riedel-de Haën), sodium chloride, potassium chloride, hydrogen chloride, sodium hydroxide, sodium bicarbonate, bile salt, calcium chloride, thiobarbituric acid, and sodium alginate (Sigma-Aldrich), trichloroacetic acid (PanReac AppliChem), 1,1,3,3-tetramethoxypropane, malondialdehyde tetrabutylammonium salt, and galacto-oligosaccharide (Danisco) of analytical grades were purchased.

Formulation of Probiotic-Fortified Camel Milk Infant Formulas

Bacterial Growth and Cell Harvesting Conditions. Bacterial growth and cell harvesting were performed as described by Poddar et al. (2014). Briefly, the probiotic strain of *L. reuteri* was inoculated in 1.5 L of sterile MRS broth, and incubated at 37°C for 18

h. After incubation, cells were harvested and centrifuged (Digicen 21 R, Ortoalresa) at 7,000 × *g* for 5 min at room temperature. The cell pellets obtained upon centrifugation were further washed twice with sterile deionized water to remove any traces of spent broth and further resuspended in sterile water to obtain a bacterial cell suspension of 10^{11} to 10^{12} cfu/mL.

Probiotic-Fortified Camel Milk Infant Formula Preparation and Spray Drying. Production of CMIF was carried out according to the USDA standards recommended for infants aged 0 to 6 mo, using a formulation developed in our previous study (Mudgil et al., 2022). Probiotic-fortified CMIF were processed according to USDA standards via calculation of the required amounts of lactose, protein, fat, multivitamins, and mineral mixtures. The total contents of protein, carbohydrate, and fat were 16%, 47%, and 37%, respectively. For vitamins, the following levels were used per 100 g of infant formula: vitamin A 525 IU, vitamin D 5 IU, vitamin E 10.5 mg, vitamin K, thiamine (vitamin B_1) 750 μg, riboflavin (vitamin B_2) 850 μg, vitamin B_6 1,000 μg, vitamin B_{12} 3 μg, niacin 10,000 μg, folic acid (folacin) 200 μg, pantothenic acid 500 μg, biotin 300 μg, vitamin C (ascorbic acid) 30 mg, choline 210 mg, and inositol 210 mg. The following levels of minerals were incorporated into the infant formula: calcium 75 mg, phosphorus 45 mg, magnesium 37.5 mg, iron 4.5 mg, zinc 7.5 mg, manganese 100 mg, copper 500 mg, iodine 150 mg, selenium 17.5 mg, sodium 50 mg, potassium 180 mg, and chloride 140 mg. To this end, CM infant formulas, as prepared in our previous study (Mudgil et al., 2022), were reconstituted in purified sterile water, labeled as **IF1** (basal infant formula), **IF2** [0.5% galacto-oligosaccharide (**GOS**)], and **IF3** [0.5% GOS and 0.5% sodium alginate (**SA**)]. Afterward, the harvested bacterial pellets were added into the 3 formulations, to approximately 10^{10} cfu/mL. To induce encapsulation, bacterial cells were mixed at room temperature using a sterile magnetic stirrer without heating for 30 min before the spray drying process. The concentration of *L. reuteri* in the infant formulas, on a dry weight basis, was 1.1% for each CMIF. The spray drying process was carried out using a pilot-scale spray drier (Mini Spray Dryer B-290, Buchi AG) with an inlet air temperature of 160°C, an outlet temperature ranging between 91 and 93°C, and a feed flow rate of 8.0 mL/min (Maciel et al., 2014). The water activity ($\mathbf{a_w}$) of IF1, IF2, and IF3 after spray drying was found to be 0.324 ± 0.003, 0.319 ± 0.006, and 0.307 ± 0.005. The moisture contents (± SD) of all 3 infant formulas were found to be 5.13 ± 0.33, 5.08 ± 0.28, and 4.96 ± 0.46 for IF1, IF2, and IF3, respectively. The whole experiment was carried out in 2 batches.

Particle Size Distribution Measurement of CMIF Fortified with L. reuteri

The particle size distribution of the *L. reuteri*-fortified CMIF samples after spray drying was determined in isopropanol with a laser light diffraction unit, using Mastersizer (Mastersizer300, Malvern Instruments). The refractive indices of the continuous phase and particles were taken as 1.333 and 1.469, respectively, as per the protocol described by Li et al. (2012).

Viability of L. reuteri Cells Under Simulated Infant Gastrointestinal Digestion

Simulated Infant Gastrointestinal Digestion Conditions. The SIGID experiments were conducted according to the method reported by (Ménard et al., 2018). Briefly, simulated gastric fluid (94 m*M* NaCl and 13 m*M* KCl, pH adjusted to 5.3 using 1 *M* HCl) and simulated intestinal juice (**SIJ**: 10 m*M* KCl, 85 m*M* $NaHCO_3$, and 164 m*M* NaCl, pH adjusted to 6.6 by 1 *M* HCl or 1 *M* NaOH) were prepared. Subsequently, 5.5 g of CMIF powder (n = 3) was added to 35 mL of warm simulated gastric fluid (40°C) in a 50-mL falcon tube, and the pH of the mixture was readjusted to 5.3 using 1 *M* HCl. To simulate infant gastric digestion (**SIGD**), a volume of 1 mL of sample aliquot was removed to enumerate viable probiotics before the treatment, and samples were kept at 4°C. Then, 1 mL of porcine pepsin (44.03 mg/mL) was added, and digestion was carried out in a water bath maintained at 37°C for 1 h under continuous shaking, and the reaction was stopped by adjusting the pH to 8.0.

After SIGD reaction time, an aliquot of 20 mL of gastric phase was withdrawn, labeled as SIGD samples, and kept at 4°C for viable cell enumerations. Thereafter, simulated intestinal digestion was induced by adding to the remaining content of gastric digesta 25 mL of SIJ containing 1 mL of $CaCl_2$ (0.332 mg/mL), 1 mL of bile salt mixture (1.2 mg/mL), 1mL of pancreatic lipase (28.57 mg/mL in SIJ), and 1 mL of pancreatin (5 mg/mL in SIJ). The pH was readjusted to 6.6 using 1 *M* NaOH. After vigorous homogenization, digestion was carried out under continuous shaking in a water bath maintained at 37°C for 60 min. To stop the intestinal digestion, heat shock treatment was applied, and samples were subjected to both simulated infant gastric and intestinal digestion phases, referred to as SIGID.

Determination of L. reuteri Cell Viability. To study the effects of SIGD and SIGID on the survivability of *L. reuteri* free and encapsulated cells in the prepared CMIF, aliquots of 1 mL from each sample were collected and serial dilutions in sterile peptone water were prepared. Following this, log cfu per gram was

determined by plating onto MRS agar for 48 h at 37°C, and *L. reuteri* free and encapsulated cells' resistance against the SIGD and SIGID conditions was calculated as follows:

$$\text{Cell viability}(\%) = \frac{\text{Log}\frac{\text{cfu}}{\text{g}} \text{ after SIGID}}{\text{Log}\frac{\text{cfu}}{\text{g}} \text{ before SIGID}} \times 100\%. \quad [1]$$

Viability of Free and Encapsulated L. reuteri Cells in CMIF Under Storage Conditions

The viability of probiotic *L. reuteri* cells in free and encapsulated forms under CMIF storage conditions was evaluated by selecting 2 storage temperatures, such as 25°C (room temperature) and 40°C (in an oven) at a relative humidity (a_w) of 0.33. In addition, 3 different relative humidity conditions, expressed in terms of water activity, such as $a_w = 0.11$ (using saturated aqueous LiCl), $a_w = 0.33$ (using saturated aqueous $MgCl_2$), and $a_w = 0.53$ [using saturated aqueous $Mg(NO_3)_2$] at room temperature (25 ± 1°C), were implemented (Weinbreck et al., 2010).

The viability analysis was conducted during a storage period of 60 d, and aliquots of 1 g of each CMIF sample were withdrawn every 15 d. In brief, log cfu per gram was determined by plating onto MRS agar after serial dilutions in sterile peptone water, and probiotic cell viability (%) was determined as per equation [1].

Physicochemical Characteristics of L. reuteri-Fortified CMIF

Caking, Color, and pH Analyses. Caking behavior of CMIF was observed visually and was recorded by taking images as described previously described by Masum et al. (2020). Powders were considered free flowing if lumps were not detected. When lumps were detected, gentle pressure was applied to them using a spatula. If the lumps could be broken down by the application of this gentle pressure, the samples were considered lumpy. In cases where the lumps could not be broken down, the samples were considered caked.

The color parameters of the different CMIF samples, expressed as **L***, **a***, and **b*** values, were determined using a HunterLab colorimeter (Color Flex EZ), where L* indicates lightness or darkness, a* is redness or greenness, and b* is yellowness or blueness (Shameh et al., 2019). In addition, pH was measured by mixing 1 g of each CMIF in 9 mL of sterile distilled water.

Effect of Storage Conditions on Lipid Oxidation Rates. The lipid oxidation of the different CMIF previously prepared was determined based on thiobarbituric acid reactive substance (**TBARS**) levels, according to the method described by Buege and Aust (1978) and later modified by Maqsood et al. (2019). To this end, a thiobarbituric acid solution was freshly prepared (100 mL, containing 0.375 g of thiobarbituric acid, 15 g of trichloroacetic acid, and 2 mL of 0.25 *N* hydrochloric acid). To determine lipid oxidation, 0.25 g of CMIF powder samples was added to 1.75 mL of thiobarbituric acid solution, vortexed for 1 min, and then heated in a water bath (100°C) for 10 min. Samples were cooled using running tap water, sonicated for 30 min, and subsequently centrifuged at 5,000 × *g* at 25°C for 10 min. Absorbances of the supernatants were recorded at 450 nm using a Thermo Scientific Multiskan Microplate Spectrophotometer, and a standard curve graph was prepared using malondialdehyde (**MDA**) stock solution as standard (1–10 μg/mL).

Scanning Electron Microscopy Analysis

The microstructure of the CMIF samples, during storage at different conditions of temperature and relative humidity, was analyzed using scanning electron microscopy. In brief, the different CMIF powders were placed on double-sided tape and gold sputter-coated (108 Auto Sputter Coater, Ted Pella Inc.), and digital images were taken using a scanning electron microscope (JSM-6010 Plus/LA scanning electron microscope, JEOL) at the desired magnification.

Fourier-Transform Infrared Analysis

Fourier-transform infrared (**FTIR**) analysis of the prepared CMIF samples, along with CM, GOS, SA and *L. reuteri* cells, was performed using an FTIR spectrometer (Spectrum Two FT-IR Spectrometer, Perkin Elmer) at d 30 and 60 of the storage period over a range of wavelengths from 450 to 4,000 cm^{-1}.

Statistical Analysis

In the present study, the different CMIF were formulated in 2 batches, and all the experiments and analyses were carried out in triplicate. Obtained data were analyzed using the one-way ANOVA and were recorded as mean ± standard deviation. Tukey's multiple comparison test was used at a level of significance of $P < 0.05$. For the statistical analysis, SPSS 26.0 software (SPSS Inc.) was used.

Table 1. Particle size distribution parameters of the control camel milk powders and the *Lactobacillus reuteri*-fortified model camel milk infant formulas (CMIF)[1]

	Particle size[2] (μm)				
Sample	Dv [10]	Dv [50]	Dv [90]	D[3,2]	D[4,3]
Camel milk powder					
CM-1	5.97 ± 0.43[c]	34.5 ± 5.25[a]	173.5 ± 6.5[a]	16.0 ± 1.35[c]	63.8 ± 3.95[a]
CM-2	0.92 ± 0.03[a]	39.4 ± 10.2[a]	1,835 ± 25[b]	3.65 ± 0.13[a]	498. ± 94.5[b]
CM-3	3.66 ± 0.12[b]	40.05 ± 2.25[a]	205 ± 2[a]	7.29 ± 0.20[b]	74.5 ± 1.9[a]
Infant formula					
IF1	1.23 ± 0.08[a]	18.5 ± 1.1[a]	223.5 ± 68.5[a]	3.84 ± 0.02[a]	117.15 ± 64.8[a]
IF2	0.94 ± 0.06[a]	21.55 ± 3.85[a]	1,375 ± 135[b]	3.53 ± 0.19[a]	275.5 ± 29.5[b]
IF3	4.33 ± 0.86[b]	42.9 ± 7.1[b]	221.5 ± 12.5[a]	8.66 ± 1.53[b]	107.4 ± 24.6[a]

[a–c]Means (n = 3) with different superscripts within a column indicate significant difference between the values within "camel milk powder" and "infant formula" ($P < 0.05$). Values are represented as mean ± SD.

[1]CM-1 = camel milk (CM) powder containing only 35% (wt/wt) CM; CM-2 = camel milk powder containing 35% CM and 0.5% galactooligosaccharide (GOS); CM-3 = camel milk powder containing 35% CM, 0.5% GOS, and 0.5% sodium alginate (SA); IF1 = *L. reuteri*-fortified CMIF containing only 35% (wt/wt) CM; IF2 = *L. reuteri*-fortified CMIF containing 35% CM and 0.5% GOS; IF3 = *L. reuteri*-fortified CMIF containing 35% CM, 0.5% GOS, and 0.5% SA.

[2]Dv[10] = volume weighted 10th percentile; Dv[50] = volume weighted 50th percentile; Dv[90] = volume weighted 90th percentile; D[3,2] = surface area moment mean; D[4,3] = volume moment weighted mean.

RESULTS AND DISCUSSION

Particle Size Distribution of the Different Models of CMIF Fortified with L. reuteri

The particle size distribution parameters of the different CM powders and the resulting CMIF (IF1, IF2, and IF3) samples after fortification with *L. reuteri* and the spray drying processing are presented in Table 1. The CM-2 powder, containing 35% CM and 0.5% GOS, displayed significantly ($P < 0.05$) higher D[4,3] (volume moment weighted mean) and Dv [90] (volume weighted 90th percentile), with respective values of 498 μm and 1,835 μm, compared with CM-1 (63.8 μm and 173.5 μm, respectively) and CM-3 (74.5 μm and 205 μm, respectively), indicating a larger average particle size (Barone et al., 2021). The same pattern was noticed with the corresponding CMIF (i.e., IF2), although the recorded values were reduced after fortification with *L. reuteri*, reaching 275.5 μm (D[4,3]) and 1,375 μm (Dv [90]; Table 1). Among the *L. reuteri*-fortified CMIF samples, the particle size, in terms of D[4,3] values, of IF3, containing CM, GOS, and SA, was the smallest (107.4 μm), followed by IF1, containing only CM (117.15 μm), whereas that of IF2 (275.5 μm) was the highest ($P < 0.05$). However, we found a nonsignificant difference between the particle size of CM-3 and the corresponding fortified CMIF (IF3; $P > 0.05$), as depicted in Table 1. The IF1 powder fortified with *L. reuteri* exhibited a significantly higher particle size compared with the CM-1 powder ($P < 0.05$). It has been reported that both composition and particle size can influence the physicochemical properties and stickiness of different dairy powders, as particle size has been shown to have a significant effect on the cohesion and adhesiveness of the powder mixtures. In fact, smaller particles with a higher specific surface area have been reported to be more susceptible to stickiness and hygroscopicity. For example, the surface composition of a skim milk powder fraction (<75 mm) displayed significantly enhanced fat (+5%) and decreased protein (−9%) coverage compared with bulk or nonfractionated sample powders (O'Donoghue et al., 2019). Moreover, the D[3,2] of the 3 IF1, IF2, and IF3 powders were 3.84, 3.53, and 8.66 μm, respectively (Table 1). For the fortified IF2 and IF3 powders, no significant changes in D[3,2] values were detected compared with the base CM powders, unlike CM-1, which showed a significant decrease in the D[3,2] value ($P < 0.05$) from 16.0 μm to 3.84 μm, after supplementation with probiotic cells (IF1), which is consistent with the observed results of Dv [50].

Viability of L. reuteri in Different CMIF Upon SIGID and During Storage

The effectiveness of the microencapsulation process of *L. reuteri* in the different CMIF was evaluated based on the percentage of cell viability after encapsulation and spray drying (Figure 1). According to the entrapment efficiency results, no significant differences in the viability of *L. reuteri* in the different matrices (IF1, IF2, and IF3) and during the spray drying processing were perceived, with encapsulation efficiencies ranging from 80 to 90%. Indeed, the drying process is considered one of the main stages of IMF powder production. Due to the quick drying and evaporative cooling, spray drying is chosen over other drying processes for producing

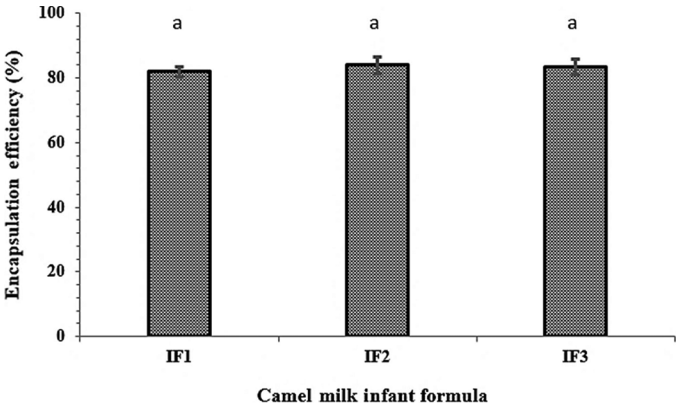

Figure 1. Encapsulation efficiency (%) of *Lactobacillus reuteri* in the different camel milk infant formulas (CMIF). IF1 = *L. reuteri*-fortified CMIF containing only 35% (wt/wt) camel milk (CM); IF2 = *L. reuteri*-fortified CMIF containing 35% CM and 0.5% galacto-oligosaccharide (GOS); IF3 = *L. reuteri*-fortified CMIF containing 35% CM, 0.5% GOS, and 0.5% sodium alginate. Means (n = 3) with different letters indicate a significant difference ($P < 0.05$). Bars represent mean ± SD.

IMF powders, causing the least levels of constituents' thermal degradation. Spray drying is further preferred because it is a highly automated sanitary process that can easily be scaled up to generate huge quantities of powders (Masum et al., 2020).

After spray drying of the different CMIF, their solubility in water was verified at ambient temperature by mixing a mass of each powder with water, and the time required for their complete solubilization was recorded (data not shown). Indeed, because IF powders are commonly reconstituted in water before use, solubility of IMF is recognized as a key functional feature. Interestingly, brief solubilization times of 12.84 ± 0.72, 14.11 ± 1.17, and 22.21 ± 1.49 s were recorded for IF1 (only CM), IF2 (CM and GOS), and IF3 (CM, GOS, and SA), respectively. This suggested good acceptably of the powders' physicochemical properties and dispersibility after spray drying. The higher time required for complete solubilization observed with IF3 might be due to the presence of both GOS and SA in the powder composition.

The viability of *L. reuteri* free and encapsulated cells in the different prepared CMIF powders under SIGD and SIGID was correspondingly investigated, and the results are summarized in Table 2. Upon undergoing SIGID, *L. reuteri* free cells revealed a significant decrement ($P < 0.05$) from 8.14 log cfu/g to 7.50 log cfu/g with 0.6 log reduction. Similarly, a significant decrease in *L. reuteri* viability from 7.61 log cfu/g to 6.93 log cfu/g with 0.6 log reduction ($P < 0.05$) was noted with IF1 powder. Meanwhile, the viability of *L. reuteri* in IF2 and IF3 was not significantly influenced by SIGD and SIGID. This can highlight the possible role of GOS and SA in the protection of probiotic cells under SGID and SIGID conditions. In addition, in comparing the viability of *L. reuteri* cells in IF2 and IF3, the addition of SA to GOS (IF3) did not show significantly greater protection of *L. reuteri* (Table 2). It has been previously reported that GOS is effective in protecting microencapsulated *Lactobacillus acidophilus* 5 and *Lactobacillus casei* 01 upon SIGD and SIGID in yogurt and orange juice samples (Krasaekoopt and Watcharapoka, 2014). Similarly, oligosaccharides, including galacto-oligosaccharide, have been found to help protect *Lactobacillus fermentum* L7 against SIGID when used as co-encapsulating agents (Liao et al., 2019). Results from the present study are therefore in line with previous literature reports, suggesting that GOS can be used as an effective protective agent for *Lactobacillus* species against SIGID conditions. Furthermore, the current findings are reporting for the first time the effectiveness of GOS in protecting probiotic bacteria fortified in camel milk-based infant formula under SIGD and SIGID environments. It is worth noting that GOS has a strong ability to inhibit lactose crystallization in hydrous matrices due to the change of lactose mutarotation (Fu et al., 2019).

The effects of different storage conditions, in terms of humidity and temperature conditions, on the sur-

Table 2. Viability of *Lactobacillus reuteri* in the different camel milk infant formula (CMIF) samples under simulated infant gastric digestion (SIGD) and simulated infant gastrointestinal digestion (SIGID)[1]

	Log cfu/g			
Condition	Free cells	IF1	IF2	IF3
Control	8.14 ± 0.07^{c}	7.61 ± 0.09^{b}	7.72 ± 0.43^{a}	7.71 ± 0.43^{a}
SIGD	7.80 ± 0.13^{b}	7.13 ± 0.10^{a}	7.53 ± 0.05^{a}	7.34 ± 0.06^{a}
SIGID	7.50 ± 0.07^{a}	6.93 ± 0.13^{a}	7.52 ± 0.09^{a}	7.26 ± 0.05^{a}

$^{a–c}$Means (n = 3) with different superscripts within a column indicate a significant difference ($P < 0.05$). Values are represented as mean ± SD.

[1]IF1 = *L. reuteri*-fortified CMIF containing only 35% (wt/wt) camel milk (CM); IF2 = *L. reuteri*-fortified CMIF containing 35% CM and 0.5% galacto-oligosaccharide (GOS); IF3 = *L. reuteri*-fortified CMIF containing 35% CM, 0.5% GOS, and 0.5% sodium alginate.

Table 3. Viability of *Lactobacillus reuteri* encapsulated in camel milk infant formula (CMIF) under different conditions of humidity (a_w = water activity) and temperature over a storage period of 60 d[1]

Formulation and storage period (d)	Log cfu/g				
	Humidity			Temperature	
	$a_w = 0.11$	$a_w = 0.33$	$a_w = 0.52$	25°C	40°C
IF1					
0	8.57 ± 0.02^{e}	8.57 ± 0.02^{d}	8.57 ± 0.02^{d}	8.57 ± 0.02^{e}	8.57 ± 0.02^{e}
15	8.27 ± 0.11^{b}	8.37 ± 0.07^{cd}	6.08 ± 0.05^{c}	5.15 ± 0.15^{c}	4.67 ± 0.04^{d}
30	8.05 ± 0.14^{b}	7.69 ± 0.06^{bc}	5.10 ± 0.05^{b}	7.20 ± 0.01^{d}	4.14 ± 0.01^{c}
45	7.92 ± 0.04^{b}	7.50 ± 0.08^{b}	4.97 ± 0.01^{b}	4.76 ± 0.04^{b}	3.35 ± 0.12^{b}
60	6.67 ± 0.06^{a}	5.49 ± 0.55^{a}	3.33 ± 0.20^{a}	3.83 ± 0.15^{a}	1.83 ± 0.24^{a}
IF2					
0	8.50 ± 0.41^{c}	8.50 ± 0.41^{c}	8.50 ± 0.41^{e}	8.50 ± 0.41^{e}	8.50 ± 0.41^{d}
15	8.28 ± 0.04^{bc}	8.62 ± 0.11^{c}	6.36 ± 0.22^{d}	5.20 ± 0.17^{c}	4.75 ± 0.08^{c}
30	7.87 ± 0.08^{b}	7.41 ± 0.10^{b}	5.30 ± 0.03^{b}	5.72 ± 0.11^{d}	2.79 ± 0.08^{ab}
45	7.85 ± 0.20^{b}	7.07 ± 0.17^{b}	5.55 ± 0.07^{c}	4.21 ± 0.30^{b}	3.52 ± 0.12^{b}
60	6.66 ± 0.04^{a}	4.46 ± 0.31^{a}	3.60 ± 0.31^{a}	3.33 ± 0.22^{a}	2.63 ± 0.55^{a}
IF3					
0	8.50 ± 0.41^{c}	8.50 ± 0.41^{d}	8.50 ± 0.41^{d}	8.50 ± 0.41^{c}	8.50 ± 0.41^{d}
15	8.27 ± 0.13^{bc}	8.24 ± 0.03^{cd}	6.79 ± 0.03^{c}	5.86 ± 0.03^{b}	4.57 ± 0.16^{c}
30	7.87 ± 0.06^{b}	7.90 ± 0.06^{c}	4.94 ± 0.05^{b}	5.45 ± 0.18^{b}	3.89 ± 0.09^{b}
45	7.87 ± 0.07^{b}	7.24 ± 0.04^{b}	5.07 ± 0.39^{b}	3.92 ± 0.07^{a}	4.32 ± 0.28^{bc}
60	6.72 ± 0.25^{a}	5.88 ± 0.08^{a}	2.26 ± 0.14^{a}	4.08 ± 0.00^{a}	2.43 ± 0.04^{a}

[a–e]Means (n = 3) with different superscripts among each formulation at each storage condition indicate a significant difference ($P < 0.05$). Values are represented as mean ± SD.

[1]IF1 = *L. reuteri*-fortified CMIF containing only 35% (wt/wt) camel milk (CM); IF2 = *L. reuteri*-fortified CMIF containing 35% CM and 0.5% galacto-oligosaccharide (GOS); IF3 = *L. reuteri*-fortified CMIF containing 35% CM, 0.5% GOS, and 0.5% sodium alginate.

vivability and stability of *L. reuteri* in the different CMIF were also investigated. As shown in Table 3, considering the effect of humidity on the viability of *L. reuteri* in IF1, cell viability decreased significantly ($P < 0.05$) through storage at the 3 different humidity conditions, from 8.57 log cfu/g to 6.67, 5.49, and 3.33 log cfu/g at humidity rates of a_w = 0.11, 0.33, and 0.52, respectively, after 60 d of storage. The same trend was observed in IF2 and IF3. Moreover, the viability of *L. reuteri* decreased as humidity levels increased. Accordingly, encapsulation was found to be ineffective in protecting *L. reuteri* under humid conditions and a long period of storage. Furthermore, a similar effect was noticed concerning the effect of temperature on *L. reuteri* viability during 60 d of storage (Table 3). Independently of the infant formula composition, cell viability in the 3 CMIF samples decreased significantly ($P < 0.05$) over the storage period, especially at higher temperature conditions (40°C), where death cycles of *L. reuteri* were higher, reaching 1.83, 2.63, and 2.43 log cfu/g, for IF1, IF2, and IF3, respectively, when stored at 40°C for 60 d.

In accordance with the current findings, oligosaccharides, including GOS, were reported, in a previous study by Liao et al. (2019), to help conserve viability of *Lactobacillus fermentum* L7 cells under long-term refrigeration storage at 4°C, when used as co-encapsulating agents. In the same context, a recent study that applied spray drying to microencapsulate *L. reuteri* TF-7 revealed that whey protein isolate and nanocrystalline starch were effective in improving the survivability and stability of the probiotic cells during long-term storage at 4, 25, and 35°C, as well as after exposure to heat and SIGID (Puttarat et al., 2021). Likewise, the effects of 16 wk of storage at 25, 4, and −18°C on the viability of encapsulated *Bifidobacterium animalis* ssp. lactis ATCC27536 and *Lactobacillus acidophilus* ATCC4356 in a conjugated whey protein hydrolysate using spray drying were studied. The mean probiotic counts of the samples before and after spray drying were 10.59 log cfu/g and 8.89 log cfu/g. After 16 wk of storage, the mean probiotic counts were 7.18 and 7.87 log cfu/g for samples stored at 4 and −18°C, respectively. In contrast, the mean probiotic counts of samples stored at 25°C significantly decreased to 3.97 log cfu/g (Minj and Anand, 2022).

Changes in the Physicochemical Characteristics of L. reuteri-Fortified CMIF During Storage

Changes in CMIF Color Under Different Storage Conditions. The effects of storage conditions (humidity and temperature) on the color features of the prepared CMIF, in terms of L*, a*, and b* coor-

dinates, were explored in the present study, and the data obtained are outlined in Table 4. It was observed that the degree of lightness in IF1 and IF3 increased significantly after storage at different humidity and temperature conditions ($P < 0.05$). The same effect was shown with IF2, except for IF2 samples stored at a relative humidity of $a_w = 0.33$ and temperature of 25°C, where the degree of increase of lightness was insignificant. Moreover, all the CMIF samples displayed a negative a* value, indicating that the greenness of samples decreased significantly after 60 d of storage under different conditions ($P < 0.05$). As well, IF1 and IF2 samples showed a greater decrease in greenness at 25°C compared with 40°C; the a* values turned positive at d 60 of storage. However, IF3 showed a greater reduction of greenness at 40°C compared with 25°C, although a* values did not turn positive at d 60 of storage. On another side of the CMIF color analysis, b* values, indicating yellowness, of all CMIF were found to be positive, with a higher degree of yellowness increment ($P < 0.05$) at 40°C compared with 25°C and at higher relative humidity levels after 60 d of storage (Table 4). Browning of milk powder during storage is associated with non-enzymatic browning reactions, such as the Maillard reaction, in which a condensation reaction takes place between a carbonyl group (e.g., from lactose) and an amino group (Xiang et al., 2021). Factors such as time, humidity, temperature, and pH can influence the Maillard reaction, and the progress of this reaction can be evaluated through color changes associated with the production of melanonids, which are responsible for brown color (Tamanna and Mahmood, 2015).

Ho et al. (2019) compared the physicochemical properties of 12 milk powders (9 different milk infant formula powders and 3 whole milk powders) and reported that b* values increased significantly after 3 mo of storage, whereas their L* values tended to decrease during the storage period. In another study, Li et al. (2019) evaluated the physicochemical properties, including color, of spray-dried camel milk powders stored at 11 to 32% relative humidity and temperature of 37°C for 18 wk. According to the findings of their study, L* and whiteness values of camel milk powder remained almost constant throughout the storage period, whereas, a* values decreased slightly and b* values increased significantly during the first 3 wk of the storage period, highlighting the influence of humidity on the b* values of milk powders and thereby reflecting the shifting of yellowness toward brown.

Changes in CMIF pH Under Different Storage Conditions. The effects of storage conditions on the physicochemical characteristics of the prepared CMIF fortified with *L. reuteri*, in terms of pH values, were analyzed, and the results are presented in Supplemental Table S1 (https://data.mendeley.com/datasets/8y8nx3c7vs; Maqsood, 2022). Humidity conditions of $a_w = 0.11$ and 0.33 showed no significant effect on the pH values of IF1, IF2, and IF3 samples after 60 d of storage. However, at higher humidity conditions ($a_w = 0.52$), the pH of CMIF increased significantly after 60 d of storage ($P < 0.05$). Storage of the different *L. reuteri*-supplemented CMIF at room temperature for 60 d did not affect the pH of IF1 and IF3, but the pH of IF2 increased significantly after 60 d of storage at room temperature. The same effect, in terms of increasing CMIF pH with longer storage period, was observed when all the CMIF (IF1, IF2, and IF3) were stored at 40°C for 60 d. The pH changes under high storage temperature and relative humidity levels can also be correlated with the previously described findings regarding CMIF color changes and attributed to the bonding of amino groups by lactose in the Maillard reaction.

Caking Behavior of CMIF During Storage. The stability of milk powder and derived product quality is known to be affected by absorbing moisture and, thereby, caking behavior. Indeed, because spray-dried milk powders are amorphous, they will quickly absorb moisture and form caked powders (Yazdanpanah and Langrish, 2013). When amorphous particles are plasticized by exposure to high temperature or humidity, or both, caking can occur (Zafar et al., 2017), and, in general, physicochemical properties decline with storage for long periods because of the hygroscopicity of amorphous lactose (Yazdanpanah and Langrish, 2013). Therefore, the effects of different storage temperature and humidity conditions on the caking parameters of the different *L. reuteri* probiotic-fortified CMIF were evaluated. As shown in Figure 2, caking of IF1 started on d 30 under different storage temperature conditions, and the largest caking size was recorded on d 60 for IF1 samples stored at 40°C, compared with IF1 samples stored at room temperature (25°C), which exhibited smaller lump sizes. Moreover, the caking behavior of IF1 samples was the lowest at $a_w = 0.11$ and $a_w = 0.33$, compared with IF1 samples stored at higher relative humidity levels ($a_w = 0.52$), which showed the highest caking parameters. Similarly, caking of IF2 samples, under different storage temperature conditions, started on the 30th day of storage, and lump size increased over the storage period when stored at 40°C, with a larger caking size on d 60 of storage. However, under different storage humidity conditions, no difference in caking behavior was perceived between IF2 samples stored at $a_w = 0.11$, 0.33, and 0.52. The same pattern, in terms of the caking parameters, was revealed by IF3 samples, under different storage temperature and humidity conditions, with caking starting on d 30 of storage, larger

Table 4. Influence of different storage humidity (a_w = water activity) and temperature conditions on the color parameters of camel milk infant formula (CMIF) over a storage period of 60 d[1]

Formulation, color parameter measured, and storage period (d)	Color parameter				
	Humidity			Temperature	
	a_w = 0.11	a_w = 0.33	a_w = 0.52	25°C	40°C
IF1					
L*					
0	93.99 ± 0.17^{a}	93.99 ± 0.17^{b}	93.99 ± 0.17^{b}	93.99 ± 0.17^{a}	93.99 ± 0.17^{b}
15	94.17 ± 0.35^{a}	91.86 ± 0.18^{a}	92.29 ± 0.33^{a}	93.77 ± 0.03^{a}	92.96 ± 0.14^{a}
30	117.38 ± 0.82^{d}	117.75 ± 0.55^{d}	116.06 ± 0.99^{d}	115.91 ± 1.42^{c}	117.63 ± 0.23^{d}
45	95.51 ± 0.01^{b}	94.33 ± 0.05^{b}	94.95 ± 0.35^{b}	95.18 ± 0.22^{a}	94.60 ± 0.51^{b}
60	101.25 ± 0.25^{c}	99.79 ± 0.94^{c}	100.96 ± 0.63^{c}	100.02 ± 1.71^{b}	100.33 ± 0.39^{c}
a*					
0	−1.42 ± 0.06^{a}	−1.42 ± 0.06^{a}	−1.42 ± 0.06^{a}	−1.42 ± 0.06^{a}	−1.42 ± 0.06^{a}
15	−1.40 ± 0.09^{a}	−1.35 ± 0.11^{ab}	−0.78 ± 0.02^{b}	−0.99 ± 0.02^{b}	−1.07 ± 0.05^{b}
30	−1.12 ± 0.14^{b}	−0.94 ± 0.01^{bc}	−0.47 ± 0.09^{c}	−0.40 ± 0.04^{c}	−0.66 ± 0.06^{c}
45	−0.96 ± 0.00^{b}	−0.78 ± 0.01^{c}	−0.37 ± 0.01^{c}	−0.53 ± 0.06^{c}	−0.61 ± 0.05^{c}
60	−1.06 ± 0.04^{b}	−0.54 ± 0.32^{c}	−0.38 ± 0.12^{c}	0.43 ± 0.15^{d}	−0.54 ± 0.09^{c}
b*					
0	6.89 ± 0.29^{c}	6.89 ± 0.29^{bc}	6.89 ± 0.29^{b}	6.89 ± 0.29^{b}	6.89 ± 0.29^{a}
15	4.20 ± 0.43^{a}	5.47 ± 1.51^{ab}	7.76 ± 0.12^{c}	5.30 ± 0.10^{a}	7.85 ± 0.05^{b}
30	7.21 ± 0.45^{c}	7.7 ± 0.12^{c}	8.04 ± 0.49^{c}	8.62 ± 0.55^{c}	9.67 ± 0.07^{c}
45	5.26 ± 0.09^{b}	4.63 ± 0.44^{a}	5.83 ± 0.12^{a}	5.56 ± 0.04^{a}	6.80 ± 0.11^{a}
60	7.63 ± 0.09^{c}	7.62 ± 0.01^{c}	9.12 ± 0.24^{d}	9.04 ± 0.06^{c}	11.13 ± 0.14^{d}
IF2					
L*					
0	93.20 ± 0.47^{a}	93.20 ± 0.47^{a}	93.20 ± 0.47^{ab}	93.20 ± 0.47^{ab}	93.20 ± 0.47^{b}
15	93.82 ± 0.74^{a}	91.33 ± 0.29^{a}	91.68 ± 0.78^{a}	93.47 ± 0.15^{ab}	90.92 ± 0.12^{a}
30	117.45 ± 0.40^{c}	146.62 ± 31.1^{b}	116.50 ± 0.85^{d}	115.4 ± 0.80^{c}	116.85 ± 0.64^{d}
45	93.89 ± 0.96^{a}	94.78 ± 0.68^{a}	93.82 ± 0.88^{b}	79.34 ± 14.9^{a}	94.18 ± 0.00^{b}
60	101.27 ± 0.23^{b}	101.20 ± 0.20^{a}	100.84 ± 0.32^{c}	98.42 ± 0.10^{bc}	99.62 ± 0.60^{c}
a*					
0	−1.31 ± 0.03^{b}	−1.31 ± 0.03^{a}	−1.31 ± 0.03^{a}	−1.31 ± 0.03^{a}	−1.31 ± 0.03^{a}
15	−1.41 ± 0.02^{a}	−1.49 ± 0.14^{a}	−0.75 ± 0.00^{b}	−0.83 ± 0.04^{b}	−0.77 ± 0.07^{b}
30	−1.06 ± 0.00^{c}	−1.05 ± 0.09^{a}	−0.32 ± 0.02^{c}	−0.24 ± 0.13^{d}	−0.50 ± 0.04^{c}
45	−0.86 ± 0.00^{d}	−0.77 ± 0.10^{a}	−0.27 ± 0.01^{c}	−0.46 ± 0.06^{c}	−0.50 ± 0.02^{c}
60	−0.80 ± 0.06^{d}	−49.4 ± 48.5^{a}	−0.41 ± 0.36^{bc}	0.36 ± 0.08^{e}	−0.13 ± 0.20^{d}
b*					
0	7.39 ± 0.07^{b}	7.39 ± 0.07^{b}	7.39 ± 0.07^{b}	7.39 ± 0.07^{b}	7.39 ± 0.07^{a}
15	5.05 ± 0.08^{a}	7.56 ± 0.25^{bc}	8.18 ± 0.04^{c}	6.87 ± 0.02^{ab}	8.74 ± 0.24^{c}
30	8.47 ± 0.01^{c}	8.36 ± 0.66^{cd}	10.00 ± 0.23^{d}	10.4 ± 0.59^{d}	10.59 ± 0.10^{d}
45	5.19 ± 0.12^{a}	5.54 ± 0.01^{a}	6.60 ± 0.35^{a}	6.59 ± 0.11^{a}	8.21 ± 0.09^{b}
60	8.38 ± 0.13^{c}	9.05 ± 0.08^{d}	9.94 ± 0.35^{d}	8.93 ± 0.04^{c}	11.13 ± 0.14^{e}
IF3					
L*					
0	92.89 ± 0.18^{a}	92.89 ± 0.18^{a}	92.89 ± 0.18^{ab}	92.89 ± 0.18^{a}	92.89 ± 0.18^{b}
15	93.87 ± 0.44^{ab}	93.27 ± 0.07^{a}	91.59 ± 0.02^{a}	93.91 ± 0.14^{ab}	90.57 ± 0.24^{a}
30	116.39 ± 1.7^{d}	117.23 ± 0.11^{d}	114.90 ± 1.80^{d}	116.57 ± 0.16^{d}	116.17 ± 1.18^{d}
45	95.05 ± 0.04^{b}	94.51 ± 0.33^{b}	94.14 ± 0.09^{b}	94.70 ± 0.09^{b}	94.20 ± 0.27^{b}
60	100.69 ± 0.06^{c}	100.15 ± 0.30^{c}	98.98 ± 0.71^{c}	100.84 ± 0.80^{c}	98.58 ± 0.89^{c}
a*					
0	−1.25 ± 0.00^{ab}	−1.25 ± 0.00^{a}	−1.25 ± 0.00^{a}	−1.25 ± 0.00^{a}	−1.25 ± 0.00^{a}
15	−1.37 ± 0.08^{a}	−0.83 ± 0.7^{ab}	−0.63 ± 0.03^{b}	−0.91 ± 0.08^{a}	−0.78 ± 0.01^{b}
30	−0.99 ± 0.14^{bc}	−0.83 ± 0.01^{ab}	−0.24 ± 0.06^{c}	−0.05 ± 0.06^{b}	−0.48 ± 0.04^{d}
45	−0.60 ± 0.17^{d}	−0.86 ± 0.03^{ab}	−0.30 ± 0.04^{c}	−0.26 ± 0.02^{b}	−0.62 ± 0.06^{c}
60	−0.77 ± 0.00^{cd}	−0.25 ± 0.40^{b}	0.14 ± 0.01^{d}	−0.20 ± 0.28^{b}	−0.12 ± 0.04^{e}
b*					
0	8.00 ± 0.06^{b}	8.00 ± 0.06^{b}	8.00 ± 0.06^{ab}	8.00 ± 0.06^{b}	8.00 ± 0.06^{ab}
15	5.75 ± 0.27^{a}	5.76 ± 0.18^{a}	9.16 ± 0.1^{bc}	6.90 ± 0.01^{a}	9.28 ± 0.22^{b}
30	8.85 ± 0.32^{c}	9.486 ± 0.13^{c}	10.00 ± 0.26^{c}	11.37 ± 0.27^{d}	10.92 ± 0.12^{c}
45	6.29 ± 0.22^{a}	6.11 ± 0.12^{a}	7.37 ± 0.43^{a}	7.25 ± 0.09^{ab}	7.78 ± 0.05^{a}
60	9.16 ± 0.18^{c}	9.28 ± 0.44^{c}	9.62 ± 1.08^{c}	10.00 ± 0.69^{c}	11.81 ± 1.12^{c}

$^{a–d}$Means (n = 6) with different superscripts among each formulation at each storage condition indicate a significant difference ($P < 0.05$). Values are represented as mean ± SD.

[1]IF1 = *Lactobacillus reuteri*-fortified CMIF containing only 35% (wt/wt) camel milk (CM); IF2 = *L. reuteri*-fortified CMIF containing 35% CM and 0.5% galacto-oligosaccharide (GOS); IF3 = *L. reuteri*-fortified CMIF containing 35% CM, 0.5% GOS, and 0.5% sodium alginate. L* indicates lightness or darkness, a* is redness or greenness, and b* is yellowness or blueness.

caking at 40°C, and no change in caking size under different storage humidity conditions (Figure 2).

Results of the prepared CMIF caking behavior are in line with results reported in previous studies. The effects of 21-d storage at different temperatures (25 and 45°C) and relative humidity levels (11, 44, and 85%) on the surface characteristics and caking behavior of IMF were explored by Phosanam et al. (2021). At higher temperatures and humidity levels, an increase in lactose crystallinity and surface fat content was observed, resulting in a change in the chemical composition of IMF and therefore a drastic increase in caking. In contrast, storage at room temperature and relatively lower humidity levels (11 and 44%) prevented lactose crystallization and caking. Another study by Phosanam et al. (2020) reported that at higher humidity levels (85%) and temperature (45°C), lactose crystallization of whole milk powder and heated skim milk powders increased, resulting in increased caking strength, more extensive Maillard reaction, and higher surface free fat. In addition, another study showed that increasing the storage temperature of infant formula to 60°C can significantly increase caking and the surface free fat content. The same study reported that fatty acids with high melting points were present on the surface of the infant formula powder, and fatty acids with low melting points remained within powder particles (Tham et al., 2017).

Effects of Storage Conditions on Lipid Oxidation of L. reuteri-Fortified CMIF. Lipid oxidation was assessed via TBARS, a measure of the formation of secondary oxidation products such as aldehydes, to understand the sensory effects of lipid oxidation. Thus, TBARS are commonly used as a marker of oxidative stress and lipid peroxidation index (Hejazy et al., 2021). Because IMF powder is prone to oxidation during storage, and thus the milk powder quality decreases, the lipid oxidation rates of the different *L. reuteri*-fortified CMIF, over 60 d of storage under different temperature and humidity conditions, in terms of TBARS value changes, were monitored, and obtained data are summarized in Table 5. On d 0, TBARS of IF-1 samples (1.88 mg equivalent MDA/kg) was higher compared with the TBARS values found in IF-2 (1.15 mg equivalent MDA/kg) and IF-3 (1.13 mg equivalent MDA/kg), due to the addition of GOS and SA in IF2 and IF3, which might have provided a protective effect around the surface of oil droplets within the formula powder, and due to which the TBARS values at d 0 were lower in IF2 and IF3.

In the present study, the different selected storage humidity and temperature conditions exhibited a significant ($P < 0.05$) effect on TBARS values and, thereby, the lipid oxidation rates of IF2 and IF3 samples over the 60-d storage period. The lipid oxidation of the CMIF samples increased significantly on d 60 of storage ($P < 0.05$), as from 1.15 mg equivalent MDA/kg to 3.43 ($a_w = 0.52$) and 4.86 (temperature of 40°C) mg equivalent MDA/kg for IF2 samples. However, at lower humidity conditions ($a_w = 0.11$ and 0.33) and room temperature (25°C) over 30 d of storage, no significant increase in the lipid oxidation levels of the CMIF was noted ($P \geq 0.05$), suggesting that microencapsulation technology can be effective to enhance CMIF at lower humidity conditions and room temperature for a short-term period (30 d). However, IF1 sample stability and lipid oxidation were not significantly affected by the different storage humidity conditions when stored at room temperature throughout the 60-d storage period. As highlighted in Table 5, only upon storage at 40°C for 60 d were the lipid oxidation rates of IF1 samples significantly affected ($P < 0.05$), with TBARS value of 3.24 mg equivalent MDA/kg, compared with 1.88 mg equivalent MDA/kg at d 0 of storage. Cheng et al. (2019) used multivariate analysis to optimize water activity for storage of high-protein and high-lipid infant formula milk powder. The results showed that the optimum water activity condition for reduced lipid oxidation was $a_w = 0.33$ for high-lipid infant formula milk powder, whereas that for high-protein infant formula milk powder was $a_w = 0.11$, which can limit the Maillard reaction.

In the same context, the effects of different storage temperature conditions (20, 28, 40, and 55°C) on the autoxidation of sealed IMF containing polyunsaturated fatty acids were analyzed for monoaldehyde levels throughout 1 yr of storage (Cesa et al., 2015). The prepared polyunsaturated fatty acid-enriched IMF were reported to be stable toward autoxidation, and thereby lipid oxidation, even at elevated temperatures. Otherwise, fortifying IMF with metal ions such as Zn, Fe, Cu, and Mn promoted reduction of rancidity through the formation of hexanal, 2-heptanone, and 2-nonaone during long-term storage of 6 mo (Wang et al., 2020). Furthermore, Li et al. (2016) investigated the effects of storage at different relative humidity levels (11–94%) on spray-dried model milk emulsions in comparison with commercial infant formula. At high relative humidity (above 50%), the models were more stable than the commercial sample, due to the presence of casein proteins that did not undergo denaturation to the same degree as the whey proteins. In addition, the presence of minerals in the commercial sample increased protein denaturation, directly affecting the elevation in browning rate.

Microstructure Analysis of L. reuteri-Supplemented CMIF. The surface morphology of CM, GOS, *L. reuteri*, and the different *L. reuteri*-supplemented

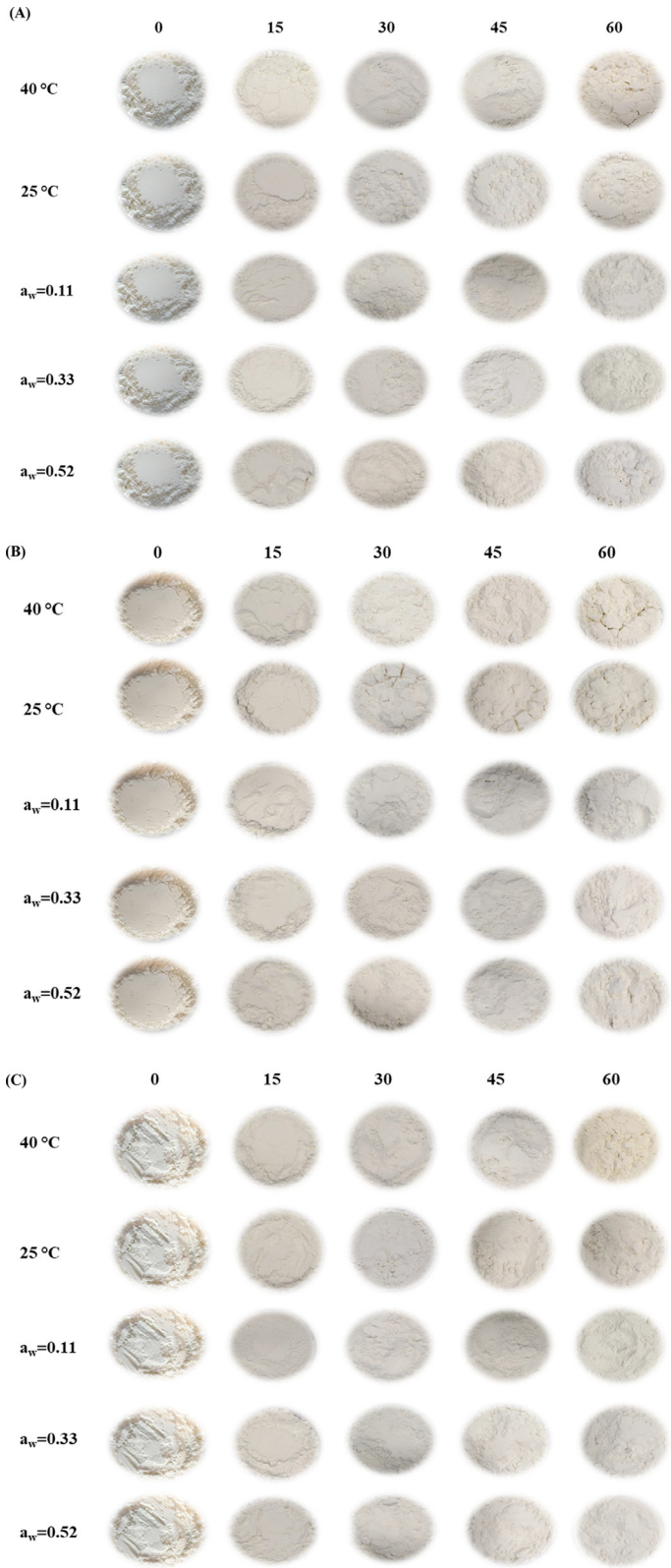

Figure 2. The effects of humidity (water activity, a_w = 0.11, 0.33, and 0.52) and temperature (25 and 40°C) conditions on the caking behavior of the different camel milk infant formulas (CMIF). (A) IF1, (B) IF2, and (C) IF3 CMIF over a storage period of up to 60 d (0, 15, 30, 45, and 60 d). IF1 = *Lactobacillus reuteri*-fortified CMIF containing only 35% (wt/wt) camel milk (CM); IF2 = *L. reuteri*-fortified CMIF containing 35% CM and 0.5% galacto-oligosaccharide (GOS); IF3 = *L. reuteri*-fortified CMIF containing 35% CM, 0.5% GOS, and 0.5% sodium alginate.

Table 5. Lipid oxidation rates [based on thiobarbituric acid reactive substance (TBARS) values] of camel milk infant formula (CMIF) under different storage humidity (a_w = water activity) and temperature conditions over a storage period of 60 d[1]

Formulation and storage period (d)	TBARS (mg equivalent MDA/kg)				
	Humidity			Temperature	
	$a_w = 0.11$	$a_w = 0.33$	$a_w = 0.52$	25°C	40°C
IF1					
0	1.88 ± 0.48^{a}	1.88 ± 0.48^{ab}	1.88 ± 0.48^{a}	1.88 ± 0.48^{ab}	1.88 ± 0.48^{a}
30	1.96 ± 0.00^{a}	1.62 ± 0.16^{a}	1.32 ± 0.19^{a}	1.57 ± 0.03^{a}	2.15 ± 0.03^{a}
60	2.03 ± 0.17^{a}	2.61 ± 0.07^{b}	1.48 ± 0.15^{a}	2.40 ± 0.02^{b}	3.24 ± 0.09^{b}
IF2					
0	1.15 ± 0.10^{a}	1.15 ± 0.10^{a}	1.15 ± 0.10^{a}	1.15 ± 0.10^{a}	1.15 ± 0.10^{a}
30	1.56 ± 0.38^{a}	1.30 ± 0.16^{a}	1.89 ± 0.08^{b}	1.80 ± 0.18^{b}	2.10 ± 0.12^{b}
60	2.41 ± 0.030^{b}	2.40 ± 0.07^{b}	3.43 ± 0.07^{c}	2.48 ± 0.19^{c}	4.86 ± 0.36^{c}
IF3					
0	1.13 ± 0.03^{a}	1.13 ± 0.03^{a}	1.13 ± 0.03^{a}	1.13 ± 0.03^{a}	1.13 ± 0.03^{a}
30	1.39 ± 0.03^{a}	1.16 ± 0.04^{a}	1.80 ± 0.03^{b}	2.65 ± 0.25^{b}	1.97 ± 0.08^{b}
60	3.80 ± 0.16^{c}	6.35 ± 0.31^{c}	5.48 ± 0.18^{c}	2.41 ± 0.25^{b}	3.20 ± 0.06^{c}

[a–c]Means (n = 3) with different superscripts among each formulation at each storage condition indicate a significant difference ($P < 0.05$). Values are represented as mean ± SD.

[1]MDA = malondialdehyde; IF1 = *Lactobacillus reuteri*-fortified CMIF containing only 35% (wt/wt) camel milk (CM); IF2 = *L. reuteri*-fortified CMIF containing 35% CM and 0.5% galacto-oligosaccharide (GOS); IF3 = *L. reuteri*-fortified CMIF containing 35% CM, 0.5% GOS, and 0.5% sodium alginate.

CMIF after spray drying and after 30 d of storage were analyzed using scanning electron microscopy technology (Figure 3). As displayed in Figure 3A, CM showed a spherical structure, and the size of milk particles was larger compared with the 3 CMIF. GOS revealed a sheet-like structure, and a road structure was observed with *L. reuteri*.

The effects of storage humidity and temperature conditions on the microstructural characteristics of the different CMIF after spray drying during a storage period of 30 d are shown in Figures 3B, C, and D. Regarding IF1 samples (Figure 3B), after spray drying and during storage at the different humidity and temperature conditions, all the samples showed a spherical and agglomerate structure. The agglomeration was higher at all the 3 humidity storage conditions. By contrast, agglomerations, large particles of sheet-like structure, and less spherical morphology were perceived with IF2 samples (Figure 3C) after spray drying and under the different storage temperatures and humidity conditions. Compared with IF1, which was concurrent to the laser diffraction particle size distribution findings, IF2 samples showed the highest particle size (Table 1). Compared with IF2, IF3 samples visibly showed less agglomeration and larger particles of sheet-like structure (Figure 3D), also in line with data of the size distribution measured by the light diffraction technique, demonstrating that the particle size was the smallest with IF3 samples (Table 1). The lower number of spherical structures and larger particles of sheet-like structure observed with IF2 and IF3 samples might be due to the presence of GOS and SA in the composition of the CMIF powders, and all the previously discussed physicochemical properties collectively determine the solubility of the different CMIF prepared in the present study. *Lactobacillus reuteri* could not be observed at higher magnification after spray drying, even in IF1 samples, which could indicate that the probiotic cells were effectively encapsulated into the CM proteins matrix.

In accordance with the current findings, Fritzen-Freire et al. (2013) used several encapsulating agents to encapsulate *Bifidobacterium* BB-12 by spray drying and found that the particles were spherical and varied in size, with concavities typical of spray-dried materials. The effects of storage at different relative humidity levels (11–94%) on spray-dried model milk emulsions compared with commercial infant formula were further investigated by Li et al. (2016). Samples stored at lower relative humidity levels (22.5%) did not undergo lactose crystallization, whereas those stored at high humidity conditions started to undergo lactose crystallization after 2 mo of storage. In addition, the appearance of their particles changed from a relatively smooth surface to a rough surface, and high agglomeration was noticed. More recently, Phosanam et al. (2020) reported that at higher humidity levels (85%), the particles of whole milk powder and heat skim milk powders became irregularly shaped due to lactose crystallization. The concentration of total solids is considered among the main factors

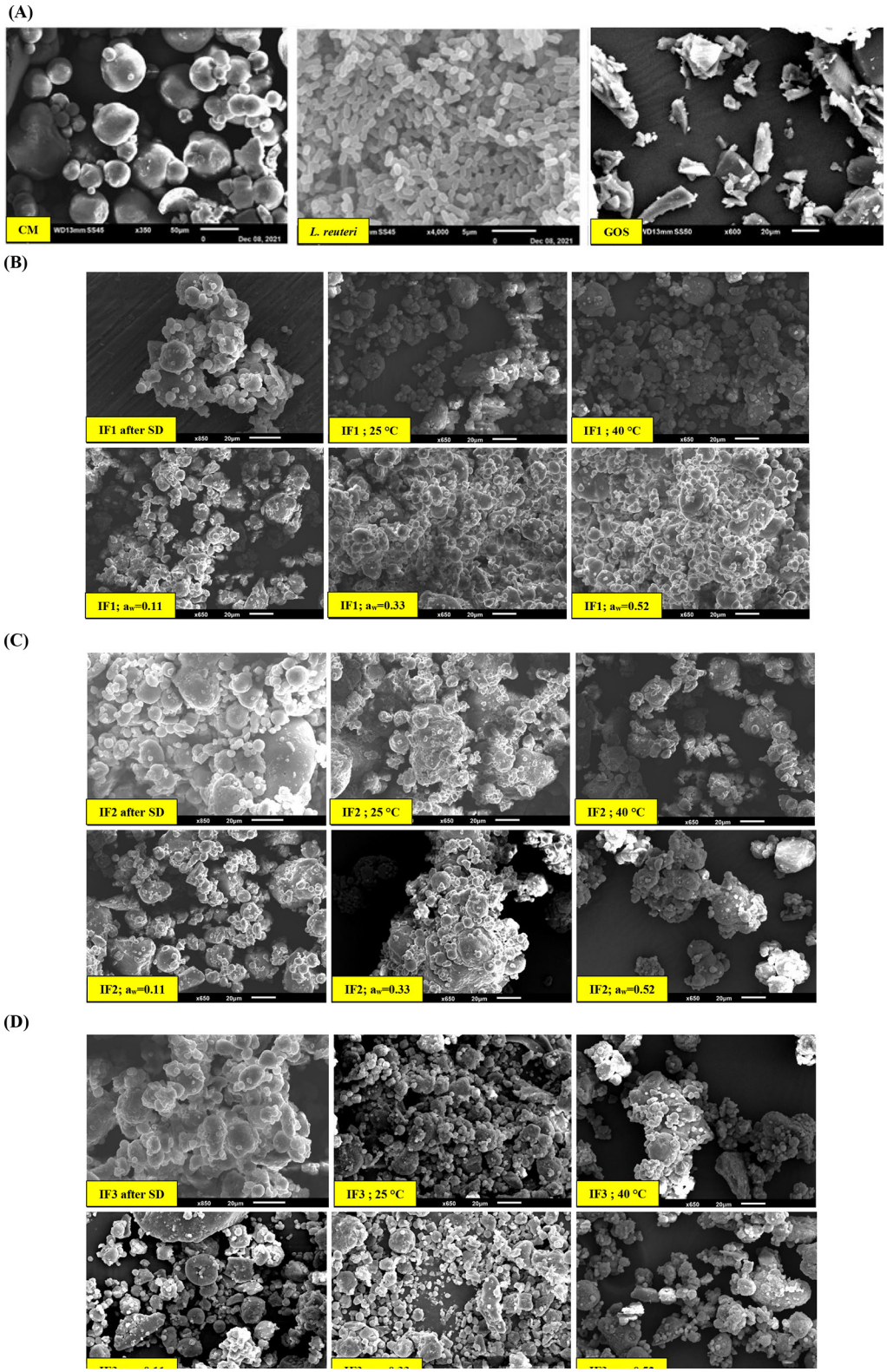

Figure 3. (A) Scanning electron microscopy images of camel milk (CM) powder, *Lactobacillus reuteri*, and galacto-oligosaccharide (GOS). Effects of storage conditions on the microstructural characteristics of the different camel milk infant formulas (CMIF): (B) IF1, (C) IF2, and (D) IF3 after a storage period of 30 d. IF1 = *L. reuteri*-fortified CMIF containing only 35% (wt/wt) camel milk (CM); IF2 = *L. reuteri*-fortified CMIF containing 35% CM and 0.5% GOS; IF3 = *L. reuteri*-fortified CMIF containing 35% CM, 0.5% GOS, and 0.5% sodium alginate. SD = spray drying.

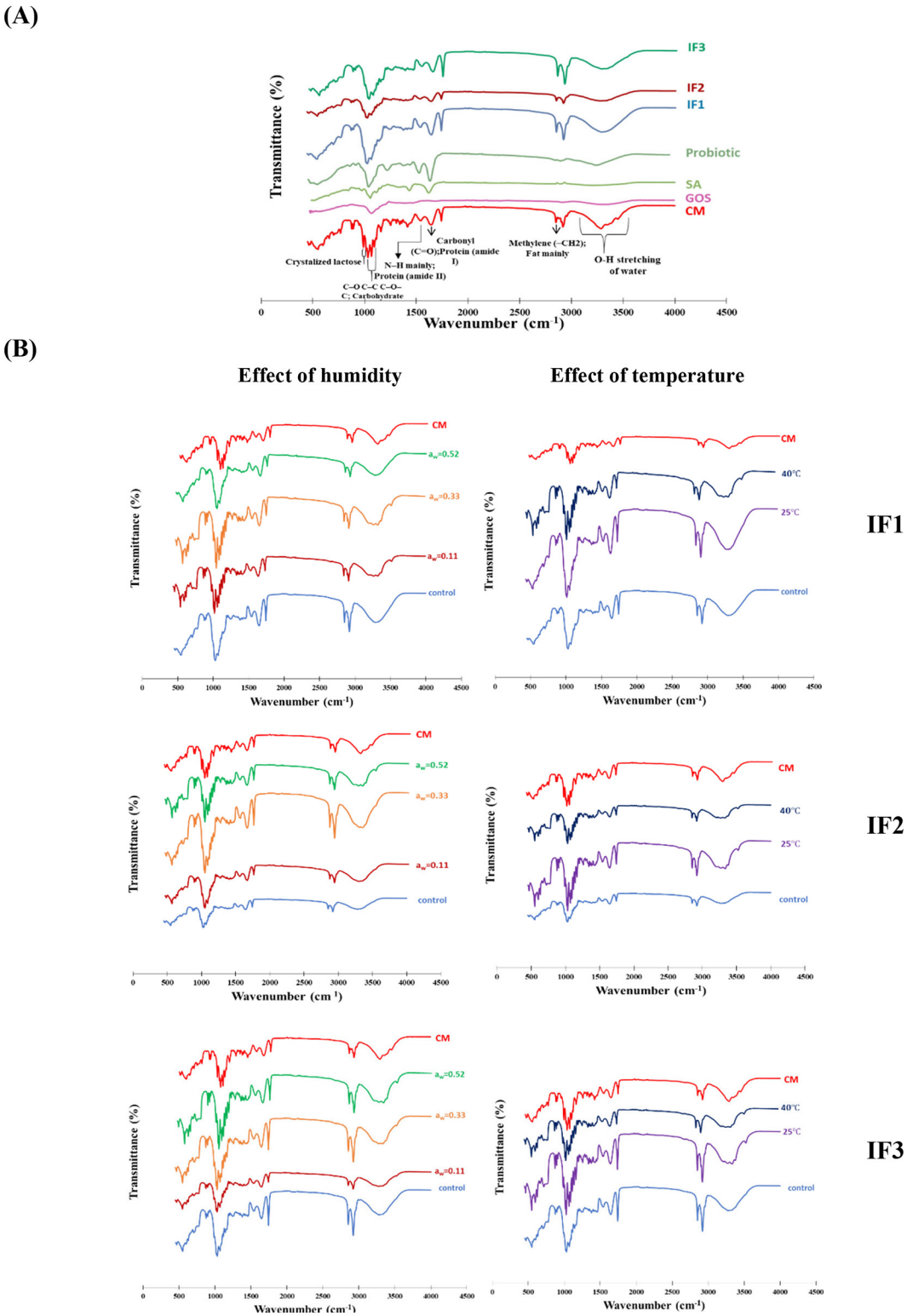

Figure 4. (A) Fourier-transform infrared (FTIR) spectra of the different camel milk infant formulas (CMIF), *Lactobacillus reuteri*, sodium alginate (SA), galacto-oligosaccharide (GOS), and camel milk (CM) powder after spray drying. (B) FTIR spectra of IF1, IF2, and IF3 after 60 d of storage under different temperature and humidity conditions, respectively. IF1 = *L. reuteri*-fortified CMIF containing only 35% (wt/wt) CM; IF2 = *L. reuteri*-fortified CMIF containing 35% CM and 0.5% GOS; IF3 = *L. reuteri*-fortified CMIF containing 35% CM, 0.5% GOS, and 0.5% SA; a_w = water activity.

that can influence the rate of crystallization (Goulart and Hartel, 2017). A study exploring the interrelationship between lactose crystallization and surface free fat of infant formula during different storage periods reported that the composition of infant formula can affect lactose crystallization, therefore influencing the amount and type of fat migration to particle surface, which causes differences in the wettability of infant formulas (Saxena et al., 2020).

FTIR Analysis of *L. reuteri*-Fortified CMIF During Storage

The FTIR spectra of CM, GOS, SA, *L. reuteri*, and the different CMIF fortified with *L. reuteri*, after spray drying, during 60 d of storage at different temperature and humidity conditions, were studied at the wavenumbers range of 450 to 4,000 cm^{-1} to detect the main components in the samples (i.e., fat, protein, lactose, and water), based on their absorption capacity of infrared radiation. Recorded spectra are shown in Figure 4. Overall, characteristic peaks of CM were present in the different CMIF after the spray drying process; in addition, peaks perceived in the GOS, the SA, and the probiotic *L. reuteri* spectra were stronger in the CMIF profiles (Figure 4A and Supplemental Table S2; (https://data.mendeley.com/datasets/8y8nx3c7vs; Maqsood, 2022).

Considering the effect of storage conditions, with 60 d of storage (Figure 4B), a new peak at the wavenumber range of 986 to 990 cm^{-1} was noticed, in both CM and the different CMIF powders. This was attributed to carbohydrate ring vibration. Furthermore, new peaks were observed in the wavenumber range of 960 to 1,200 cm^{-1} and were attributed to crystallized lactose (Lei et al., 2010). Crystalline lactose takes much longer than amorphous lactose to dissolve in water. However, during CMIF storage at a relative humidity of $a_w = 0.11$, fewer changes in the functional groups' distinct fingerprint features were perceived, compared with the CMIF samples stored at higher humidity levels ($a_w = 0.33$ and $a_w = 0.52$) and temperatures (40°C). This corroborates well with the previously described findings regarding color, pH, caking behavior, and lipid oxidation rate changes in the different CMIF during storage at different temperature and humidity conditions.

Few studies have used FTIR spectroscopy analysis to investigate physicochemical changes in milk during storage under different conditions. Grewal et al. (2017) reported that milk samples stored at high temperatures (40 and 50°C) showed remarkable differences in the FTIR bands that correspond to milk lipid conformations and the intermolecular β-sheet of proteins, suggesting protein-lipid interactions and aggregation. Furthermore, Li et al. (2016) demonstrated, according to their FTIR analysis results, that the spray-dried infant formula samples conserved their native form without undergoing denaturation after 6 mo of storage under different conditions (relative humidity of 22, 57, and 84%), unlike the commercial infant formula sample, which experienced protein denaturation.

CONCLUSIONS

In the present study, 3 different CMIF were produced by spray drying processing, using different matrices models to encapsulate *L. reuteri* probiotic cells (CM, GOS, and SA). The encapsulation technology interestingly showed effectiveness in protecting *L. reuteri* during the harsh conditions of SIGD and SIGID. In addition, *L. reuteri* displayed better viability and stability when stored at lower humidity and temperature conditions. Higher humidity and temperature conditions were found to significantly affect the physicochemical characteristics of the prepared CMIF, in terms of decreased greenness, and increase of yellowness and whiteness, and further increased caking occurrence and heightened lipid oxidation rates, considering TBARS values. Further research is needed to support the viability of *L. reuteri* and to improve the stability of CMIF by studying other storage conditions and encapsulation materials. In addition, detailed sensory analysis is required for further development of this product.

ACKNOWLEDGMENTS

The authors thank United Arab Emirates University (Al Ain) for funding this research through a strategic grant (Zayed Center of Health Science Fund Code:12R116) awarded to principal investigator Sajid Maqsood. The authors have not stated any conflicts of interest.

REFERENCES

Ali Redha, A., H. Valizadenia, S. A. Siddiqui, and S. Maqsood. 2022. A state-of-art review on camel milk proteins as an emerging source of bioactive peptides with diverse nutraceutical properties. Food Chem. 373(Pt A):131444.

Barone, G., J. O'Regan, A. L. Kelly, and J. A. O'Mahony. 2021. Calcium fortification of a model infant milk formula system using soluble and insoluble calcium salts. Int. Dairy J. 117:104951. https://doi.org/10.1016/j.idairyj.2020.104951.

Binda, S., C. Hill, E. Johansen, D. Obis, B. Pot, M. E. Sanders, A. Tremblay, and A. C. Ouwehand. 2020. Criteria to qualify microorganisms as "probiotic" in foods and dietary supplements. Front. Microbiol. 11:1662. https://doi.org/10.3389/fmicb.2020.01662.

Buege, J. A., and S. D. Aust. 1978. Microsomal lipid peroxidation. Pages 302–310 in Methods in Enzymology. Vol. 52. S. Fleischer and L. Packer, ed. Academic Press.

Byrne, M. E., J. A. O'Mahony, and T. F. O'Callaghan. 2021. Compositional and functional considerations for bovine-, caprine- and

ARTICLE IN PRESS

plant-based infant formulas. Dairy 2:695–715. https://doi.org/10.3390/dairy2040054.

Cesa, S., M. A. Casadei, F. Cerreto, and P. Paolicelli. 2015. Infant milk formulas: Effect of storage conditions on the stability of powdered products towards autoxidation. Foods 4:487–500. https://doi.org/10.3390/foods4030487.

Cheng, H., H. Erichsen, J. Soerensen, M. A. Petersen, and L. H. Skibsted. 2019. Optimising water activity for storage of high lipid and high protein infant formula milk powder using multivariate analysis. Int. Dairy J. 93:92–98. https://doi.org/10.1016/j.idairyj.2019.02.008.

Chi, C., Y. Xue, R. Liu, Y. Wang, N. Lv, H. Zeng, N. Buys, B. Zhu, J. Sun, and C. Yin. 2020. Effects of a formula with a probiotic *Bifidobacterium lactis* supplement on the gut microbiota of low birth weight infants. Eur. J. Nutr. 59:1493–1503. https://doi.org/10.1007/s00394-019-02006-4.

Fritzen-Freire, C. B., E. S. Prudêncio, S. S. Pinto, I. B. Muñoz, and R. D. Amboni. 2013. Effect of microencapsulation on survival of *Bifidobacterium* BB-12 exposed to simulated gastrointestinal conditions and heat treatments. Lebensm. Wiss. Technol. 50:39–44. https://doi.org/10.1016/j.lwt.2012.07.037.

Fu, S., S. Miao, X. Ma, T. Ding, X. Ye, and D. Liu. 2019. Inhibition of lactose crystallisation in the presence of galacto-oligosaccharide. Food Hydrocoll. 88:127–136. https://doi.org/10.1016/j.foodhyd.2018.09.043.

Goulart, D. B., and R. W. Hartel. 2017. Lactose crystallization in milk protein concentrate and its effects on rheology. J. Food Eng. 212:97–107. https://doi.org/10.1016/j.jfoodeng.2017.05.012.

Grewal, M. K., J. Chandrapala, O. Donkor, V. Apostolopoulos, L. Stojanovska, and T. Vasiljevic. 2017. Fourier transform infrared spectroscopy analysis of physicochemical changes in UHT milk during accelerated storage. Int. Dairy J. 66:99–107. https://doi.org/10.1016/j.idairyj.2016.11.014.

Hejazy, M., S. A. Khatibi, and Z. Shamsi. 2021. The effect of frying process on the level of malondialdehyde in different meat products. J. Nutr. Food Security 6:367–373. https://doi.org/10.18502/jnfs.v6i4.7621.

Hill, C., F. Guarner, G. Reid, G. R. Gibson, D. J. Merenstein, B. Pot, L. Morelli, R. B. Canani, H. J. Flint, S. Salminen, P. C. Calder, and M. E. Sanders. 2014. The International Scientific Association for Probiotics and Prebiotics consensus statement on the scope and appropriate use of the term probiotic. Nat. Rev. Gastroenterol. Hepatol. 11:506–514. https://doi.org/10.1038/nrgastro.2014.66.

Ho, T. M., S. Chan, A. J. E. Yago, R. Shravya, B. R. Bhandari, and N. Bansal. 2019. Changes in physicochemical properties of spray-dried camel milk powder over accelerated storage. Food Chem. 295:224–233. https://doi.org/10.1016/j.foodchem.2019.05.122.

Kaźmierczak-Siedlecka, K., G. Roviello, M. Catalano, and K. Polom. 2021. Gut microbiota modulation in the context of immune-related aspects of *Lactobacillus* spp. and *Bifidobacterium* spp. in gastrointestinal cancers. Nutrients 13:2674. https://doi.org/10.3390/nu13082674.

Krasaekoopt, W., and S. Watcharapoka. 2014. Effect of addition of inulin and galactooligosaccharide on the survival of microencapsulated probiotics in alginate beads coated with chitosan in simulated digestive system, yogurt and fruit juice. Lebensm. Wiss. Technol. 57:761–766. https://doi.org/10.1016/j.lwt.2014.01.037.

Lei, R., X. Chai, H. Mei, H. Zhang, Y. Chen, and Y. Sun. 2010. Four divalent transition metal carboxyarylphosphonate compounds: Hydrothermal synthesis, structural chemistry and generalized 2D FTIR correlation spectroscopy studies. J. Solid State Chem. 183:1510–1520. https://doi.org/10.1016/j.jssc.2010.04.037.

Li, J., A. Ye, S. J. Lee, and H. Singh. 2012. Influence of gastric digestive reaction on subsequent in vitro intestinal digestion of sodium caseinate-stabilized emulsions. Food Funct. 3:320–326. https://doi.org/10.1039/c2fo10242k.

Li, K., M. W. Woo, and C. Selomulya. 2016. Effects of composition and relative humidity on the functional and storage properties of spray dried model milk emulsions. J. Food Eng. 169:196–204. https://doi.org/10.1016/j.jfoodeng.2015.09.002.

Li, Y. H., W. J. Wang, L. Guo, Z. P. Shao, and X. J. Xu. 2019. Comparative study on the characteristics and oxidation stability of commercial milk powder during storage. J. Dairy Sci. 102:8785–8797. https://doi.org/10.3168/jds.2018-16089.

Liao, N., B. Luo, J. Gao, X. Li, Z. Zhao, Y. Zhang, Y. Ni, and F. Tian. 2019. Oligosaccharides as co-encapsulating agents: effect on oral *Lactobacillus fermentum* survival in a simulated gastrointestinal tract. Biotechnol. Lett. 41:263–272. https://doi.org/10.1007/s10529-018-02634-6.

Maciel, G. M., K. S. Chaves, C. R. Grosso, and M. L. Gigante. 2014. Microencapsulation of *Lactobacillus acidophilus* La-5 by spray-drying using sweet whey and skim milk as encapsulating materials. J. Dairy Sci. 97:1991–1998. https://doi.org/10.3168/jds.2013-7463.

Maldonado, J., M. Gil-Campos, J. Maldonado-Lobón, M. Benavides, K. Flores-Rojas, R. Jaldo, I. Jiménez Del Barco, V. Bolívar, A. Valero, E. Prados, I. Peñalver, and M. Olivares. 2019. Evaluation of the safety, tolerance and efficacy of 1-year consumption of infant formula supplemented with *Lactobacillus fermentum* CECT5716 Lc40 or *Bifidobacterium breve* CECT7263: A randomized controlled trial. BMC Pediatr. 19:361. https://doi.org/10.1186/s12887-019-1753-7.

Maqsood, S. 2022. Lactobacillus reuteri fortified camel milk infant formula: Effect of encapsulation, in-vitro digestion and storage conditions on probiotic viability and physicochemical characteristics. Mendeley Data, V1. https://doi.org/10.17632/8y8nx3c7vs.1.

Maqsood, S., A. Al-Dowaila, P. Mudgil, H. Kamal, B. Jobe, and H. M. Hassan. 2019. Comparative characterization of protein and lipid fractions from camel and cow milk, their functionality, antioxidant and antihypertensive properties upon simulated gastro-intestinal digestion. Food Chem. 279:328–338. https://doi.org/10.1016/j.foodchem.2018.12.011.

Markowiak, P., and K. Slizewska. 2017. Effects of probiotics, prebiotics, and synbiotics on human health. Nutrients 9:1021. https://doi.org/10.3390/nu9091021.

Martin, C. R., P. R. Ling, and G. L. Blackburn. 2016. Review of infant feeding: Key features of breast milk and infant formula. Nutrients 8:279. https://doi.org/10.3390/nu8050279.

Masum, A. K. M., J. Chandrapala, T. Huppertz, B. Adhikari, and B. Zisu. 2020. Effect of storage conditions on the physicochemical properties of infant milk formula powders containing different lactose-to-maltodextrin ratios. Food Chem. 319:126591. https://doi.org/10.1016/j.foodchem.2020.126591.

Ménard, O., C. Bourlieu, S. C. De Oliveira, N. Dellarosa, L. Laghi, F. Carrière, F. Capozzi, D. Dupont, and A. Deglaire. 2018. A first step towards a consensus static in vitro model for simulating full-term infant digestion. Food Chem. 240:338–345. https://doi.org/10.1016/j.foodchem.2017.07.145.

Minj, S., and S. Anand. 2022. Development of a spray-dried conjugated whey protein hydrolysate powder with entrapped probiotics. J. Dairy Sci.10520382048

Momen, S., M. Salami, F. Alavi, Z. Emam-Djomeh, and A. A. Moosavi-Movahedi. 2019. The techno-functional properties of camel whey protein compared to bovine whey protein for fabrication a model high protein emulsion. Lebensm. Wiss. Technol. 101:543–550. https://doi.org/10.1016/j.lwt.2018.11.063.

Motalebi Moghanjougi, Z., M. Rezazadeh Bari, M. Alizadeh Khaledabad, S. Amiri, and H. Almasi. 2021. Microencapsulation of *Lactobacillus acidophilus* LA-5 and *Bifidobacterium animalis* BB-12 in pectin and sodium alginate: A comparative study on viability, stability, and structure. Food Sci. Nutr. 9:5103–5111. https://doi.org/10.1002/fsn3.2470.

Mudgil, P., W. N. Baba, M. Alneyadi, A. Ali Redha, and S. Maqsood. 2022. Production, characterization, and bioactivity of novel camel milk-based infant formula in comparison to bovine and commercial sources. Lebensm. Wiss. Technol. 154:112813. https://doi.org/10.1016/j.lwt.2021.112813.

Muthukumaran, M. S., P. Mudgil, W. N. Baba, M. A. Ayoub, and S. Maqsood. 2022. A comprehensive review on health benefits, nutritional composition and processed products of camel milk. Food Rev. Int. 2022:1–37. https://doi.org/10.1080/87559129.2021.2008953.

O'Donoghue, L. T., M. K. Haque, D. Kennedy, F. R. Laffir, S. A. Hogan, J. A. O'Mahony, and E. G. Murphy. 2019. Influence of particle size on the physicochemical properties and stickiness of dairy powders. Int. Dairy J. 98:54–63. https://doi.org/10.1016/j.idairyj.2019.07.002.

Phosanam, A., J. Chandrapala, T. Huppertz, B. Adhikari, and B. Zisu. 2021. Changes in physicochemical and surface characteristics in model infant milk formula powder (IMF) during storage. Dry. Technol. 39:2119–2129. https://doi.org/10.1080/07373937.2020.1755978.

Phosanam, A., J. Chandrapala, T. Huppertz, B. Adhikari, and B. Zisu. 2020. Effect of storage conditions on physicochemical and microstructural properties of skim and whole milk powders. Powder Technol. 372:394–403. https://doi.org/10.1016/j.powtec.2020.06.020.

Poddar, D., S. Das, G. Jones, J. Palmer, G. B. Jameson, R. G. Haverkamp, and H. Singh. 2014. Stability of probiotic *Lactobacillus paracasei* during storage as affected by the drying method. Int. Dairy J. 39:1–7. https://doi.org/10.1016/j.idairyj.2014.04.007.

Puttarat, N., S. Thangrongthong, K. Kasemwong, P. Kerdsup, and M. Taweechotipatr. 2021. Spray-drying microencapsulation using whey protein isolate and nano-crystalline starch for enhancing the survivability and stability of *Lactobacillus reuteri* TF-7. Food Sci. Biotechnol. 30:245–256. https://doi.org/10.1007/s10068-020-00870-z.

Savarino, G., A. Corsello, and G. Corsello. 2021. Macronutrient balance and micronutrient amounts through growth and development. Ital. J. Pediatr. 47:109. https://doi.org/10.1186/s13052-021-01061-0.

Saxena, J., B. Adhikari, R. Brkljaca, T. Huppertz, J. Chandrapala, and B. Zisu. 2020. Inter-relationship between lactose crystallization and surface free fat during storage of infant formula. Food Chem. 322:126636. https://doi.org/10.1016/j.foodchem.2020.126636.

Shameh, S., A. Alirezalu, B. Hosseini, and R. Maleki. 2019. Fruit phytochemical composition and color parameters of 21 accessions of five *Rosa* species grown in North West Iran. J. Sci. Food Agric. 99:5740–5751. https://doi.org/10.1002/jsfa.9842.

Tamanna, N., and N. Mahmood. 2015. Food processing and Maillard reaction products: Effect on human health and nutrition. Int. J. Food Sci. 2015:526762. https://doi.org/10.1155/2015/526762.

Terpou, A., A. Papadaki, I. K. Lappa, V. Kachrimanidou, L. A. Bosnea, and N. Kopsahelis. 2019. Probiotics in food systems: Significance and emerging strategies towards improved viability and delivery of enhanced beneficial value. Nutrients 11:1591. https://doi.org/10.3390/nu11071591.

Tham, T. W. Y., X. Xu, A. T. H. Yeoh, and W. Zhou. 2017. Investigation of caking by fat bridging in aged infant formula. Food Chem. 218:30–39. https://doi.org/10.1016/j.foodchem.2016.09.043.

Vandenplas, Y., A. Analitis, C. Tziouvara, A. Kountzoglou, A. Drakou, M. Tsouvalas, A. Mavroudi, and I. Xinias. 2017. Safety of a new synbiotic starter formula. Pediatr. Gastroenterol. Hepatol. Nutr. 20:167–177. https://doi.org/10.5223/pghn.2017.20.3.167.

Walsh, C., J. A. Lane, D. van Sinderen, and R. M. Hickey. 2020. Human milk oligosaccharides: Shaping the infant gut microbiota and supporting health. J. Funct. Foods 72:104074. https://doi.org/10.1016/j.jff.2020.104074.

Wang, W., Y. Li, L. Cai, and L. Fang. 2020. Characteristics on the oxidation stability of infant formula powder with different ingredients during storage. Food Sci. Nutr. 8:6392–6400. https://doi.org/10.1002/fsn3.1928.

Wazed, M. A., and M. Farid. 2022. Denaturation kinetics and storage stability of Osteopontin in reconstituted infant milk formula. Food Chem. 379:132138. https://doi.org/10.1016/j.foodchem.2022.132138.

Weinbreck, F., I. Bodnar, and M. L. Marco. 2010. Can encapsulation lengthen the shelf-life of probiotic bacteria in dry products? Int. J. Food Microbiol. 136:364–367. https://doi.org/10.1016/j.ijfoodmicro.2009.11.004.

Xiang, J., F. Liu, B. Wang, L. Chen, W. Liu, and S. Tan. 2021. A literature review on Maillard reaction based on milk proteins and carbohydrates in food and pharmaceutical products: Advantages, disadvantages, and avoidance strategies. Foods 10:1998. https://doi.org/10.3390/foods10091998.

Yao, M., J. Xie, H. Du, D. J. McClements, H. Xiao, and L. Li. 2020. Progress in microencapsulation of probiotics: A review. Compr. Rev. Food Sci. Food Saf. 19:857–874. https://doi.org/10.1111/1541-4337.12532.

Yazdanpanah, N., and T. A. G. Langrish. 2013. Comparative study of deteriorative changes in the ageing of milk powder. J. Food Eng. 114:14–21. https://doi.org/10.1016/j.jfoodeng.2012.07.026.

Zafar, U., V. Vivacqua, G. Calvert, M. Ghadiri, and J. A. S. Cleaver. 2017. A review of bulk powder caking. Powder Technol. 313:389–401. https://doi.org/10.1016/j.powtec.2017.02.024.

Zhang, Y. J., S. Li, R. Y. Gan, T. Zhou, D. P. Xu, and H. B. Li. 2015. Impacts of gut bacteria on human health and diseases. Int. J. Mol. Sci. 16:7493–7519. https://doi.org/10.3390/ijms16047493.

Zibaee, S., S. M. Hosseini, M. Yousefi, A. Taghipour, M. A. Kiani, and M. R. Noras. 2015. Nutritional and therapeutic characteristics of camel milk in children: A systematic review. Electron. Physician 7:1523–1528. https://doi.org/10.19082/1523.

Zou, Z., J. A. Duley, D. M. Cowley, S. Reed, B. J. Arachchige, P. Koorts, P. N. Shaw, and N. Bansal. 2022. Digestibility of proteins in camel milk in comparison to bovine and human milk using an in vitro infant gastrointestinal digestion system. Food Chem. 374:131704. https://doi.org/10.1016/j.foodchem.2021.131704.

ORCIDS

Priti Mudgil https://orcid.org/0000-0003-0809-485X
Marwa Hamdi https://orcid.org/0000-0002-3375-8497
Ali Ali Redha https://orcid.org/0000-0002-9665-9074
Tholkappiyan Ramachandran https://orcid.org/0000-0001-6729-5227
Fathala Hamed https://orcid.org/0000-0001-7191-2136
Sajid Maqsood https://orcid.org/0000-0003-2099-8392